J|A|C|S ARTICLES

Published on Web 08/13/2010

Transition State Models for Probing Stereoinduction in Evans Chiral Auxiliary-Based Asymmetric Aldol Reactions

C. B. Shinisha and Raghavan B. Sunoj*

Department of Chemistry, Indian Institute of Technology Bombay, Powai, Mumbai 400076, India

Received March 7, 2010; E-mail: sunoj@chem.iitb.ac.in

Abstract: The use of chiral auxiliaries is one of the most fundamental protocols employed in asymmetric synthesis. In the present study, stereoselectivity-determining factors in a chiral auxiliary-based asymmetric aldol reaction promoted by $TiCl_4$ are investigated by using density functional theory methods. The aldol reaction between chiral titanium enolate [derived from Evans propionyl oxazolidinone (**1a**) and its variants oxazolidinethione (**1b**) and thiazolidinethione (**1c**)] and benzaldehyde is examined by using transition-state modeling. Different stereochemical possibilities for the addition of titanium enolates to aldehyde are compared. On the basis of the coordination of the carbonyl/thiocarbonyl group of the chiral auxiliary with titanium, both pathways involving nonchelated and chelated transition states (TSs) are considered. The computed relative energies of the stereoselectivity-determining C−C bond formation TSs in the nonchelated pathway, for both **1a** and **1c**, indicate a preference toward Evans *syn* aldol product. The presence of a ring carbonyl or thiocarbonyl group in the chiral auxiliary renders the formation of neutral $TiCl_3$-enolate, which otherwise is energetically less favored as compared to the anionic $TiCl_4$-enolate. Hence, under suitable conditions, the reaction between titanium enolate and aldehyde is expected to be viable through chelated TSs leading to the selective formation of non-Evans *syn* aldol product. Experimentally known high stereoselectivity toward Evans *syn* aldol product is effectively rationalized by using the larger energy differences between the corresponding diastereomeric TSs. In both chelated and nonchelated pathways, the attack by the less hindered face of the enolate on aldehyde through a chair-like TS with an equatorial disposition of the aldehydic substituent is identified as the preferred mode. The steric hindrance offered by the isopropyl group and the possible chelation are identified as the key reasons behind the interesting stereodivergence between Evans and non-Evans products normally reported for the title reaction. The application of an *activation strain model* on the critical TSs has been effective toward rationalizing the origin of stereoselectivity. Improved interaction energy between the reactants is found to be the key stabilizing factor for the lowest energy TS in both chelated and nonchelated pathways. The present study provides newer insights on the role of titanium(IV) toward modulating stereoselectivity in aldol reactions.

Introduction

Asymmetric induction by using covalent incorporation of chiral auxiliaries is a widely employed strategy in organic synthesis. Oxazolidinones, popularly known as Evans chiral auxiliaries, originally developed for efficient C−C bond construction in an asymmetric fashion, are a classic example of chiral auxiliary-based stereoinduction.[1] The ability of acylated oxazolidinones to engage in chelation with metal ions, along with the steric shielding of one of the enolate faces (due to the presence of suitable substituents at the fourth position oxazolidinone ring, Scheme 1), gives versatility to this group of chiral auxiliaries.[2] Over the years, application of oxazolidinone and its variants as chiral auxiliaries has continued to gain increased prominence in organic synthesis.[3]

Scheme 1. Possible Stereoisomeric Products Resulting from an Oxazolidinone-Mediated Aldol Reaction between a Titanium Enolate (**I**) and an Aldehyde

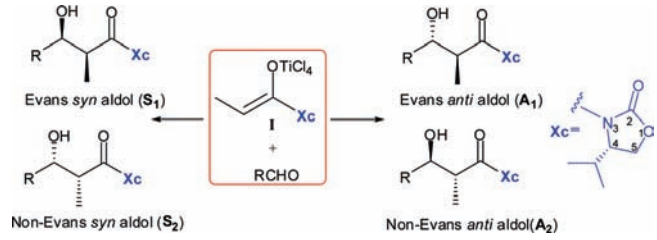

(1) (a) Evans, D. A.; Bartroli, J.; Shih, T. L. *J. Am. Chem. Soc.* **1981**, *103*, 2127. (b) Evans, D. A. *Aldrichim. Acta* **1982**, *15*, 23. (c) Abdel-Magid, A.; Pridgen, L. N.; Eggleston, D. S.; Lantos, I. *J. Am. Chem. Soc.* **1986**, *108*, 4595. (d) Ager, D. J.; Prakash, I.; Schaad, D. R. *Aldrichim. Acta* **1997**, *30*, 3. (e) Phoon, C. W.; Abell, C. *Tetrahedron Lett.* **1998**, *39*, 2655. (f) Evans, D. A.; Helmchen, G.; Rüping, M. In *Asymmetric Synthesis—The Essentials*; Christmann, M., Bräse, S., Eds.; Wiley-VCH & Co.: Weinheim, 2007; Vol. 3.

(2) (a) Evans, D. A.; Rieger, D. L.; Bilodeau, M. T.; Urpi, F. *J. Am. Chem. Soc.* **1991**, *113*, 1047. (b) Chiral *N*-propionyloxazolidinone is shown in Figure S1 of the Supporting Information.

(3) (a) Cosp, A.; Romea, P.; Talavera, P.; Urpi, F.; Vilarrasa, J.; Font-Bardia, M.; Solans, X. *Org. Lett.* **2001**, *3*, 615. (b) Evans, D. A.; Starr, J. T. *Angew. Chem., Int. Ed.* **2002**, *41*, 1787. (c) Zhang, Y.; Sammakia, T. *Org. Lett.* **2004**, *6*, 3139. (d) Crimmins, M. T.; Christie, H. S.; Chaudhary, K.; Long, A. *J. Am. Chem. Soc.* **2005**, *127*, 13810. (e) Patel, J.; Clavé, G.; Renard, P.-Y.; Franck, X. *Angew. Chem., Int. Ed.* **2008**, *47*, 4224. (f) Tessier, A.; Lahmar, N.; Pytkowicz, J.; Briguad, T. *J. Org. Chem.* **2008**, *73*, 2621. (g) Crimmins, M. T.; King, B. W. *J. Am. Chem. Soc.* **1998**, *120*, 9084.

Scheme 2. Illustration of Stereodivergence in *syn*-Aldol Reactions through Chelated and Nonchelated Transition States

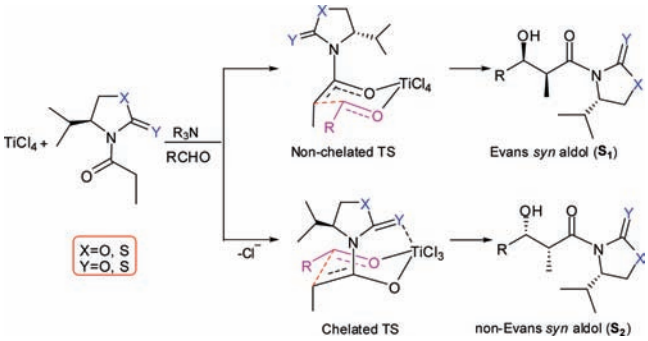

Asymmetric aldol reactions using chiral auxiliaries are indeed one of the quintessential examples,[4] wherein chiral titanium or boron enolates are typically produced. The addition of chiral metal enolates thus generated to suitable electrophiles can result in different stereoisomeric products, as shown in Scheme 1. The original studies on oxazolidinone as chiral auxiliary in titanium- or boron-promoted reactions reported the formation of Evans *syn* aldol product with high diastereoselectivity.[5] Titanium enolates are also known to yield non-Evans *syn* aldol product, presumably through a chelation-controlled pathway.[6] Other factors such as the nature of the bound ligands are known to influence the stereochemical outcome of oxazolidinone-mediated aldol reactions using titanium enolates.[7] The generation of *anti* aldol products is now increasingly available in more recent literature.[8]

A closer perusal of related literature conveys that the stereochemical outcome of asymmetric aldol reactions using Evans chiral auxiliary protocol is delicately dependent on the nature of the auxiliary group. For instance, changing the carbonyl of oxazolidinone to a thiocarbonyl group can alter the product stereochemistry. In the early 1990s, Yan et al. noticed opposite facial selectivity preferences in the aldol reaction of a variety of electrophiles with chlorotitanium enolates of camphor-based *N*-propionyloxazolidinethione and *N*-propionyloxazolidinone. The former afforded non-Evans *syn* aldol products, while the latter resulted in Evans *syn* aldol products.[9] Crimmins and co-workers also reported the change in stereoselectivity from Evans *syn* aldol to non-Evans *syn* aldol when the chiral auxiliary was changed from oxazolidinone (**1a**) to thiazolidinethione (**1c**). A description of Evans and non-Evans aldol products is provided in Scheme 2. The formation of Evans or non-Evans *syn* aldol adducts when oxazolidinethione and thiazolidinethione are used as the chiral auxiliary is reported to depend on the nature and quantity of the base employed in the reaction.[10,11] The selectivity toward Evans *syn* aldol or non-Evans *syn* aldol products is also known to depend on the bulkiness of the aldehyde.[14a] It has been proposed that increasing the chelation potential of the enolate ligand could lead to modulation of facial selectivity promoted by the chelation effect. The improved nucleophilicity of thiazolidinethione has also been suggested to result in a highly ordered chelated transition state (TS), albeit without any verification. The ligands bound to the titanium center are also found to be efficient in promoting π-facial differentiation.[2a,12] The stereochemical differences that result upon varying the reaction conditions with these chiral auxiliaries are also exploited in organic synthesis.[3d,13]

Qualitative models have thus far been adopted to explain the molecular origin of stereoselectivity in these reactions.[12,14] Since hexacoordinate arrangement is one of the preferred modes of coordination in titanium Lewis acids, it is reasonable to expect that the reaction may proceed through an open TS or through a chelated complex resulting from the displacement of chloride ions. The nonchelated TS models are generally employed to explain the formation of Evans *syn* aldol product. In this model, titanium coordinates with the enolate oxygen and the carbonyl group of the approaching aldehyde. The formation of non-Evans *syn* aldol product, on the other hand, is usually accounted for by invoking a chelated TS model. The Lewis acidity of Ti(IV) permits chelation with the oxazolidinone carbonyl, thereby leading to a conformational change of the oxazolidinone ring as compared to the nonchelated model (Scheme 2). As a result, the change in the orientation of the isopropyl group in the chelated TS will have a direct bearing on the stereochemical outcome of the reaction.[13]

Though the above-mentioned models of chiral auxiliary-based stereoselective aldol reactions are widely employed toward rationalizing the observed selectivities, a clear picture of the stereoselectivity-controlling TSs is seldom reported.[15] In this article, we present the results of a comprehensive investigation on Evans chiral auxiliary-based asymmetric aldol reaction, where titanium salts are used as the Lewis acid. We have examined different possible modes, involving both chelated and nonchelated pathways, to establish the factors that control the stereochemical course of this fundamentally important reaction. The key TSs are identified that are responsible for the formation of four stereochemically important products. Another key objective is to examine the role of a heteroatom on the chiral auxiliary. To address these issues, competing chelated and nonchelated TSs for an aldol reaction using three different chiral

(4) (a) Palomo, C.; Oiarbide, M.; García, J. M. *Chem. Soc. Rev.* **2004**, *33*, 65. (b) Davies, S. G.; Garner, A. C.; Roberts, P. M.; Smith, A. D.; Sweet, M. J.; Thomson, J. E. *Org. Biomol. Chem.* **2006**, *4*, 2753.

(5) Details of the stereochemical descriptions and nomenclature employed here are in accordance with the standard practices found in the current literature. Further details are provided on page S2 of Supporting Information.

(6) Bonner, M. P.; Thornton, E. R. *J. Am. Chem. Soc.* **1991**, *113*, 1299.

(7) Shirodkar, S.; Nerz-Stormes, M.; Thornton, E. R. *Tetrahedron Lett.* **1990**, *31*, 4699.

(8) (a) Evans, D. A.; Tedow, J. S.; Shaw, J. T.; Downey, C. W. *J. Am. Chem. Soc.* **2002**, *124*, 392. (b) Evans, D. A.; Downey, C. W.; Shaw, J. T.; Tedow, J. S. *Org. Lett.* **2002**, *4*, 1127. (c) Crimmins, M. T.; McDougall, P. J. *Org. Lett.* **2003**, *5*, 591. (d) Hajra, S.; Giri, A. K.; Karmakar, A.; Khatua, S. *Chem. Commun.* **2007**, *23*, 2408.

(9) (a) Yan, T.-H.; Tan, C.-W.; Lee, H.-C.; Lo, H.-C.; Huang, T.-Y. *J. Am. Chem. Soc.* **1993**, *115*, 2613. (b) Yan, T.-H.; Lee, H.-C.; Tan, C.-W. *Tetrahedron Lett.* **1993**, *34*, 3559.

(10) (a) Crimmins, M. T.; King, B. W.; Tabet, E. A. *J. Am. Chem. Soc.* **1997**, *119*, 7883. (b) Crimmins, M. T.; Chaudhary, K. *Org. Lett.* **2000**, *2*, 775. (c) Crimmins, M. T.; King, B. W.; Tabet, E. A.; Chaudhary, K. *J. Org. Chem.* **2001**, *66*, 894.

(11) Evans, D. A.; Shaw, J. T. *Act. Chim.* **2003**, 35.

(12) Nerz-Stormes, M.; Thornton, E. R. *Tetrahedron Lett.* **1986**, *27*, 897.

(13) Zhang, W.; Carter, R. G.; Yokochi, A. F. T. *J. Org. Chem.* **2004**, *69*, 2569.

(14) (a) Nerz-Stormes, M.; Thornton, E. R. *J. Org. Chem.* **1991**, *56*, 2489. (b) Siegel, C.; Thornton, E. R. *J. Am. Chem. Soc.* **1989**, *111*, 5722. (c) Crimmins, M. T.; Shamszad, M. *Org. Lett.* **2007**, *9*, 149.

(15) A few examples for Zimmerman−Traxler-type transition-state models for aldol reactions have been reported: (a) Li, Y.; Paddon-Row, M. N.; Houk, K. N. *J. Am. Chem. Soc.* **1988**, *110*, 3684. (b) Li, Y.; Paddon-Row, M. N.; Houk, K. N. *J. Org. Chem.* **1990**, *55*, 481.

auxiliaries such as oxazolidinone, oxazolidinethione, and thiazolidinethione are considered.

Computational Methods

Geometry optimizations of all key stationary points were carried out in the gas phase at the B3LYP (L1),[16] mPW1K (L2),[17] mPW1PW91 (L3),[18] M05-2X (L5),[19] and B98 (L6)[20] levels of theory by using the Gaussian 03 and Gaussian 09 suites of quantum chemical programs.[21] These functionals are frequently used in contemporary literature for addressing various situations where reaction barrier heights are calculated.[22] For all atoms, the 6-31G* basis set is employed for geometry optimization. We have also examined the effect of using a different basis set on titanium at the B3LYP level, by choosing the Los Alamos pseudopotential basis set (LANL2DZ), while the rest of the elements were treated by using the 6-31G* basis set (L4).[23,24] The geometries of the critical TSs were again optimized at the levels of theory L1−L6 by using a more flexible basis set (6-311G**), and single-point energies were then evaluated by including diffuse functions. The single-point energies on the optimized geometries were also evaluated by using the dispersion-corrected DFT-D (L7)[25] method as implemented in the ORCA quantum chemical package (B3LYP-D).[26]

All stationary points on the respective potential energy surfaces were characterized at the same levels of theory by evaluating the corresponding Hessian indices. Careful verification of the unique imaginary frequencies for the TSs has been carried out to examine whether the frequency indeed pertains to the desired reaction coordinate. Further, intrinsic reaction coordinate calculations were carried out to authenticate the TSs.[27] Single-point energies were calculated at the respective levels of theory using a more flexible triple-ζ-quality basis set, including polarization functions on the hydrogen atoms along with diffuse functions on non-hydrogen atoms (6-311+G** (with 6d functions)). The solvent effects were then incorporated with the continuum solvation model using the SCRF-PCM framework. Dichloromethane (DCM) was taken as the continuum solvent dielectric ($\varepsilon = 8.93$) since it has been used as solvent previously in these kinds of reactions.[8,28] The energy in solution ($G_{solvation}$, denoted as E in the text) is comprised of the electronic energy of the polarized solute and the electrostatic solute−solvent interaction energy. The solvent effects in the case of the DFT-D method (L7) are included at the same level of theory by using the COSMO solvation model.[29] We have focused on the stereoselectivity-controlling C−C bond formation step as well as on the relative energies of the crucial diastereomeric TSs. The relative energies are reported with respect to the lowest energy TS in respective cases.

Terminology. The terms "chelated" and "nonchelated" transition states respectively refer to coordination by the ring carbonyl (or thiocarbonyl) group of oxazolidinone (or oxazolidinethione/thiazolidinethione) with the metal center. In the chelated pathway, one of the metal coordination site is occupied by the carbonyl oxygen, while in the nonchelated form, the coordination site is saturated by a chloride ion (Scheme 2). The letters **S** and **A** are used to represent the TS leading respectively to *syn* and *anti* aldol products. The subscripts **1** and **2** respectively correspond to Evans and non-Evans products. The TSs $\mathbf{S_1}$, $\mathbf{S_2}$, $\mathbf{A_1}$, and $\mathbf{A_2}$ therefore correspond to Evans *syn*, non-Evans *syn*, Evans *anti*, and non-Evans *anti* products.[5] In the nonchelated TSs, additional descriptors ***a*** and ***s*** indicate the orientation of the carbonyl group of the chiral auxiliary with respect to the enolate carbonyl as *anti* and *syn*, respectively. The chelated TSs are represented by a prime after the product descriptors, e.g., $\mathbf{TS\text{-}S_1'}$.

Results and Discussion

The aldol reaction between benzaldehyde and acyl derivatives of different chiral auxiliaries such as oxazolidinone (**1a**), oxazolidinethione (**1b**), and thiazolidinethione (**1c**) with $TiCl_4$ as Lewis acid is chosen for the present investigation, with an objective to unravel the molecular origin of stereoselectivity. The asymmetric carbon (C_4 position) of the auxiliary with an isopropyl group is retained in the *S* configuration in this study.[1a] All critical transition states and intermediates that directly influence the stereochemical course of the reaction are identified by using DFT, and their stereoelectronic features are analyzed in detail.

The $TiCl_4$-promoted enolization process has been studied previously by using both ^1H and ^{13}C NMR spectroscopic methods.[30] The computed energies in the present study indicate that the *Z*-enolates are 2−3 kcal/mol more stable than the corresponding *E*-enolates.[31] The experimental reports on aldol reactions of *N*-acyloxazolidinones indicate that the stereoselectivities are consistent with the involvement of *Z*-enolates.[32] The evidence for the existence of enolate in the *Z*-configuration received further support from NMR spectroscopic as well as isotopic labeling studies.[33] Examples are also available wherein the isomeric purity of enolate intermediates could be confirmed by X-ray crystallography conducted on suitably trapped enolates.[6] Hence, in the present study, we have primarily focused on the aldol reaction of *Z*-enolates.[34]

The aldehyde and the titanium *Z*-enolate offer prochiral faces and give rise to two key modes of approach between them.

(16) (a) Becke, A. D. *J. Chem. Phys.* **1993**, *98*, 5648. (b) Becke, A. D. *Phys. Rev. A* **1998**, *38*, 3098. (c) Lee, C.; Yang, W.; Parr, R. G. *Phys. Rev. A* **1998**, *37*, 785.

(17) (a) Lynch, B. J.; Fast, P. L.; Harris, M.; Truhlar, D. G. *J. Phys. Chem. A* **2000**, *104*, 4811. (b) Lynch, B. J.; Zhao, Y.; Truhlar, D. G. *J. Phys. Chem. A* **2003**, *107*, 1384.

(18) Adamo, C.; Barone, V. *J. Chem. Phys.* **1998**, *108*, 664.

(19) Zhao, Y.; Schultz, N. E.; Truhlar, D. G. *J. Chem. Theory. Comput.* **2006**, *2*, 364.

(20) Becke, A. D.; Schmider, H. L. *J. Chem. Phys.* **1998**, *108*, 9624.

(21) (a) Frisch, M. J.; et al. *Gaussian 03*, Revisions C.02 and E.01; Gaussian, Inc.: Wallingford, CT, 2004. (b) Frisch, M. J.; et al. *Gaussian 09*, Revision A.02; Gaussian, Inc.: Wallingford, CT, 2009.

(22) (a) Lynch, B. J.; Fast, P. L.; Harris, M.; Truhlar, D. G. *J. Phys. Chem. A* **2000**, *104*, 4811. (b) Lynch, B. J.; Truhlar, D. G. *J. Phys. Chem. A* **2001**, *105*, 2936. (c) Curtiss, L. A.; Redfern, P. C.; Raghavachari, K. *J. Chem. Phys.* **2005**, *123*, 124107. (d) Wheeler, S. E.; Moran, A.; Pieniazek, S. N.; Houk, K. N. *J. Phys. Chem. A* **2009**, *113*, 10376. (e) Patel, C.; Sunoj, R. B. *J. Org. Chem.* **2010**, *75*, 359.

(23) (a) Ditchfield, R.; Hehre, W. J.; Pople, J. A. *J. Chem. Phys.* **1971**, *54*, 724. (b) Hehre, W. J.; Ditchfield, R.; Pople, J. A. *J. Chem. Phys.* **1972**, *56*, 2257. (c) Hariharan, P. C.; Pople, J. A. *Theor. Chim. Acta* **1973**, *28*, 213.

(24) (a) Hay, P. J.; Wadt, W. R. *J. Chem. Phys.* **1985**, *82*, 270. (b) Hay, P. J.; Wadt, W. R. *J. Chem. Phys.* **1985**, *82*, 299.

(25) (a) Grimme, S. *J. Comput. Chem.* **2004**, *25*, 1463. (b) Grimme, S. *J. Comput. Chem.* **2006**, *27*, 1787.

(26) Neese, F. *ORCA—An Ab Initio, Density Functional and Semiemperical Program Package*; University of Bonn: Bonn, Germany, 2007.

(27) Gonzalez, C.; Schlegel, H. B. *J. Chem. Phys.* **1989**, *90*, 2154.

(28) Evans, D. A.; Urpi, F.; Somers, T. C.; Clark, J. S.; Bilodeau, M. T. *J. Am. Chem. Soc.* **1990**, *112*, 8215.

(29) Sinnecker, S.; Rajendran, A.; Klamt, A.; Diedenhofen, M.; Neese, F. *J. Phys. Chem. A* **2006**, *110*, 2235.

(30) Mechanistic studies on titanium-promoted enolization of α-hydroxy ketones have been reported: Moreira, I. de P. R.; Bofill, J. M.; Anglada, J. M.; Solsona, J. G.; Nebot, J.; Romea, P.; Urpi, F. *J. Am. Chem. Soc.* **2008**, *130*, 3242.

(31) The energy difference as well as the optimized geometries of enolates is provided in Figure S2 in the Supporting Information.

(32) Itoh, Y.; Yamanaka, M.; Mikami, K. *J. Am. Chem. Soc.* **2004**, *126*, 13174.

(33) Kimball, D. B.; Michalczyk, R.; Moody, E.; Ollivault-Shiflett, M.; Jesus, K. D.; Silks, L. A., III *J. Am. Chem. Soc.* **2003**, *125*, 14666.

(34) However, the reaction of titanium *E*-enolate with benzaldehyde for representative cases through chelated as well as nonchelated pathways has also been examined. The selectivity is found to be toward Evans *anti* aldol, and the results are tabulated in Table S1 in the Supporting Information.

Scheme 3. Important Modes of Addition of Titanium Enolate to Benzaldehyde in the Nonchelated Pathway with the Ring Carbonyl/Thiocarbonyl Group Oriented Either *anti* (I) or *syn* (II) with Respect to the Enolate Oxygen: View along the Incipient C−C Bond (Reaction Coordinate)

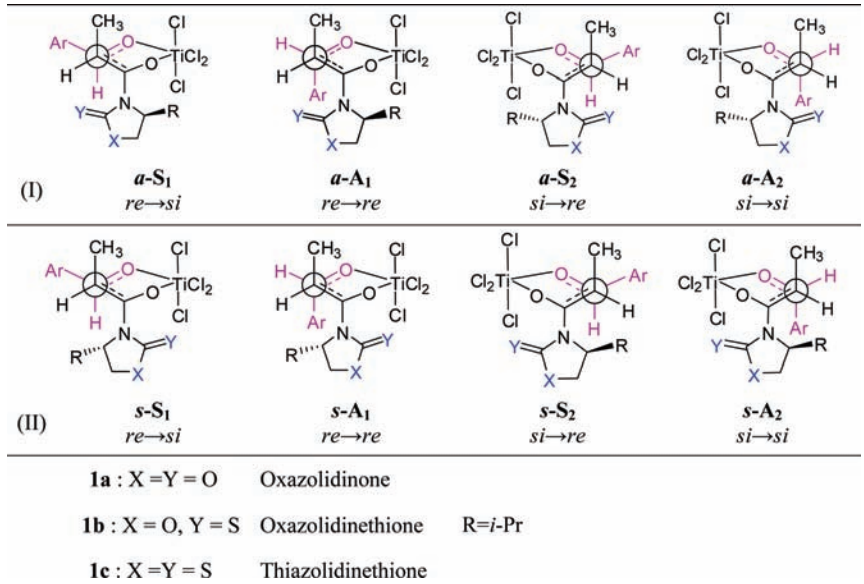

Depending on the orientation of the chiral auxiliary, additions by both the hindered and unhindered faces of the *Z*-enolate of *N*-propionyl derivatives of **1a** and **1b** as well as **1c** on the *si*/*re* face of benzaldehyde are considered. In these cases, both chelated and nonchelated pathways are examined as well. Coordination of the carbonyl (or thiocarbonyl) group with the titanium is present in the former, while it is absent in the latter, wherein the oxazolidinone ring is away from the metal center. These stereochemical possibilities can lead to unique diastereomeric products. Three important questions demand immediate attention: (a) What is the most favored mode of addition between the enolate and the electrophile? (b) What are the relative preferences between different pathways responsible for stereochemically different products? (c) What are the contributing stereoelectronic factors operating in the corresponding TSs? These questions are addressed in the following manner. A prereacting complex (PRC) is envisaged first, wherein the C═O group of the incoming electrophile (benzaldehyde) coordinates to the titanium atom. Coordination from the carbonyl oxygens of the enolate and the electrophile results in a hexacoordinate titanium complex. The number of possible conformers for such complexes is therefore restricted. A schematic diagram representing important nonchelated TSs for C−C bond formation between titanium *Z*-enolate and benzaldehyde is provided in Scheme 3. An additional model, as shown in Scheme 3-II, wherein the oxazolidinone ring is oriented differently with respect to the enolate oxygen, is additionally examined. Such reorientation within the nonchelated model can give rise to different conformers. In the first set of approaches, depicted as $\mathbf{S_{1\ or\ 2}}$ and $\mathbf{A_{1\ or\ 2}}$, the orientation of the ring carbonyl (or thiocarbonyl) is *anti* with respect to the enolate oxygen, while in the additional set, the corresponding orientation is *syn*. The modes of approach leading to products $\mathbf{S_1}$ and $\mathbf{A_1}$ involve the attack of the enolate through its unhindered face on benzaldehyde, ***a*-S$_1$** and ***a*-A$_1$** as shown in Scheme 3-I. The corresponding representations are ***s*-S$_1$** and ***s*-A$_1$** for the additional possibility (Scheme 3-II).

All key nonchelated TSs for the C−C bond formation are first located. The carbonyl groups of the enolate as well as benzaldehyde are found to maintain coordination with the titanium center in the optimized geometries. The relative energies of these TSs with respect to the lowest energy TS are given in Table 1. In the nonchelated TS model, attack by the less hindered *re* face of enolate on the *si* face of benzaldehyde is found to be energetically the most favored approach. In this mode of addition, the ring carbonyl orientation is *anti* to the enolate oxygen. The geometry of **TS-*a*-S$_1$**, as provided in Figure 1, reveals that the methyl group and the developing alkoxide oxygen (which would eventually be the new −OH group) are on the same side, evidently suggesting the formation of Evans *syn* aldol product. Interestingly, the computed relative energies of the TSs for chiral auxiliaries **1a**−**c** indicate a preference toward Evans *syn* aldol product. It is of additional significance at this juncture to note that the computed relative energies of TSs obtained at different levels of theory are in very good mutual agreement (Table 1). With larger differences in the energies of the competing diastereomeric TSs, higher levels of stereoselectivity can be expected with these chiral auxiliaries.

The optimized geometries of the diastereomeric TSs for the C−C bond formation reaction are provided in Figure 1.[35] The stereoelectronic features of these TSs are carefully examined to establish the factors that could influence the stereochemical outcome of the reaction. Some of the pertinent details are summarized here. The incipient C−C bond lengths (reaction coordinate) in **TS-*a*-S$_1$** (2.33 Å) indicate a tighter TS as compared to **TS-*a*-A$_2$** (2.42 Å). The geometric features of *syn* TSs, namely, **TS-*a*-S$_1$** and **TS-*a*-S$_2$**, indicate a chair-like geometry, whereas *anti* TSs, **TS-*a*-A$_1$** and **TS-a-A$_2$**, present a boat-like conformer. The substituents around the developing C−C bond in the higher energy boat-like TSs, such as in **TS-*a*-A$_1$** and **TS-*a*-A$_2$**, tend to remain eclipsed (d2 = −13° and 12°) as compared to the lower energy chair-like **TS-*a*-S$_1$** and **TS-*a*-S$_2$**, wherein the substituents maintain a staggered orientation (d2 = −66° and 69°, Figure 1-I). Similar torsional preferences of the substituents around the developing bond are

(35) The optimized TS geometries for chiral auxiliaries oxazolidinethione and thiazolidinethione are provided in Figure S4 in the Supporting Information.

Table 1. Computed Relative Energies[a] (in kcal/mol) of Important Transition States in the Nonchelated Pathway Obtained at Various Levels of Theory[b] for the Addition of Titanium Enolate to Benzaldehyde

transition state	mode of approach	relative energies						
		L1	L2	L3	L4	L5	L6	L7
				Oxazolidinone (**1a**)				
TS-a-S$_1$	*re*→*si*	**0.0**	**0.0**	**0.0**	**0.0**	**0.0**	**0.0**	**0.0**
		(0.0)	(0.0)	(0.0)	(0.0)	(0.0)	(0.0)	(0.0)
TS-a-A$_1$	*re*→*re*	3.2	5.1	5.6	3.4	5.8	3.9	5.8
		(3.2)	(10.3)	(6.6)	(3.6)	(6.6)	(3.9)	(7.0)
TS-a-S$_2$	*si*→*re*	4.6	5.6	6.5	4.7	6.8	4.9	6.0
		(5.2)	(11.9)	(7.6)	(5.1)	(7.6)	(6.1)	(7.2)
TS-a-A$_2$	*si*→*si*	6.0	7.9	8.0	6.2	8.6	5.9	7.0
		(7.9)	(9.7)	(9.8)	(5.9)	(10.4)	(8.4)	(8.9)
TS-s-S$_1$	*re*→*si*	9.5	8.9	13.2	10.3	10.8	11.6	9.3
		(16.9)	(15.4)	(20.9)	(17.5)	(18.6)	(17.0)	(17.3)
TS-s-A$_1$	*re*→*re*	12.4	12.1	10.0	12.8	10.8	14.2	12.7
		(19.8)	(18.5)	(18.0)	(20.3)	(22.3)	(19.6)	(20.3)
TS-s-S$_2$	*si*→*re*	8.5	13.9	8.5	11.6	8.6	9.7	7.8
		(14.6)	(21.6)	(15.4)	(17.9)	(15.8)	(15.0)	(15.0)
TS-s-A$_2$	*si*→*si*	11.1	10.5	11.6	9.2	12.2	12.7	11.3
		(17.2)	(18.3)	(18.2)	(15.2)	(18.6)	(17.6)	(17.7)
				Oxazolidinethione (**1b**)				
TS-a-S$_1$	*re*→*si*	**0.0**	**0.0**	**0.0**	**0.0**	**0.0**	**0.0**	**0.0**
		(0.0)	(0.0)	(0.0)	(0.0)	(0.0)	(0.0)	(0.0)
TS-a-A$_1$	*re*→*re*	4.0	5.8	5.0	4.2	5.9	4.1	6.9
		(3.8)	(6.8)	(9.3)	(4.1)	(7.0)	(3.5)	(7.8)
TS-a-S$_2$	*si*→*re*	4.2	5.3	4.6	4.3	6.6	4.7	5.4
		(4.8)	(6.5)	(5.7)	(4.8)	(7.5)	(5.2)	(6.7)
TS-a-A$_2$	*si*→*si*	5.7	7.6	5.7	6.0	8.3	6.0	6.6
		(7.3)	(9.4)	(7.4)	(7.4)	(9.7)	(7.2)	(8.4)
TS-s-S$_1$	*re*→*si*	11.1	12.6	10.9	11.8	12.7	12.6	11.2
		(17.6)	(15.9)	(17.5)	(18.3)	(20.6)	(17.8)	(18.7)
TS-s-S$_2$	*si*→*re*	8.8	9.6	8.2	9.6	8.5	9.9	8.3
		(14.2)	(19.9)	(14.0)	(14.7)	(16.1)	(14.0)	(14.9)
				Thiazolidinethione (**1c**)				
TS-a-S$_1$	*re*→*si*	**0.0**	**0.0**	**0.0**	**0.0**	**0.0**	**0.0**	**0.0**
		(0.0)	(0.0)	(0.0)	(0.0)	(0.0)	(0.0)	(0.0)
TS-a-A$_1$	*re*→*re*	4.1	6.1	5.4	4.2	5.8	5.2	7.1
		(4.0)	(7.2)	(4.9)	(5.5)	(7.4)	(6.8)	(7.8)
TS-a-S$_2$	*si*→*re*	2.0	4.8	4.0	3.3	6.1	3.9	4.6
		(3.9)	(6.5)	(4.7)	(5.0)	(7.8)	(4.6)	(6.0)
TS-a-A$_2$	*si*→*si*	5.1	7.3	6.3	5.2	7.9	4.2	6.3
		(6.4)	(9.4)	(7.3)	(6.6)	(10.1)	(4.0)	(7.8)
TS-s-S$_2$	*si*→*re*	—[c]	8.6	8.1	—[c]	7.6	8.5	7.2
			(15.5)	(16.2)		(14.8)	(12.7)	(13.5)

[a] L1 = PCM$_{(DCM)}$/B3LYP/6-311+G**//B3LYP/6-31G*; L2 = PCM$_{(DCM)}$/mPW1K/6-311+G**//mPW1K/6-31G*; L3 = PCM$_{(DCM)}$/mPW1PW91/6-311+G**//mPW1PW91/6-31G*; L4 = PCM$_{(DCM)}$/B3LYP/LANL2DZ (Ti), 6-311+G**//B3LYP/LANL2DZ(Ti),6-31G* for all other atoms; L5 = PCM$_{(DCM)}$/M05-2X/6-311+G**//M05-2X/6-31G*; L6 = PCM$_{(DCM)}$/B98/6-311+G**//B98/6-31G*; L7 = COSMO$_{(DCM)}$/B3LYP-D/6-311+G**//B3LYP/6-31G*. [b] Gas-phase relative energies at the respective levels of theory are given in parentheses. [c] The TS at the levels of theory of L1 and L4 could not be located after repeated attempts.

found to influence the stereoselectivity in a variety of reactions.[36] The dihedral angles describing the orientation of (i) the oxazolidinone ring with respect to the enolate double bond (d1) and (ii) the substituents around the developing C−C bond (d2) are provided in Figure 1. In the lower energy TSs (**TS-*a*-S$_1$** and **TS-*a*-A$_1$**), the oxazolidinone ring tends to remain in-plane with the enolate moiety (d1 = −162° and −179°), whereas out-of-plane arrangement is noticed for the higher energy TSs (**TS-*a*-S$_2$** and **TS-*a*-A$_2$**, d1 = −136° and −139°). In both *anti* TSs (**A$_1$** and **A$_2$**), the phenyl group of benzaldehyde and the oxazolidinone ring of the enolate are found to remain in a 1,3-*cis* disposition. The 1,3-destabilizing interaction in this situation is minimized in the boat conformer.[37] However, these groups are farther apart in the TSs responsible for *syn* aldol products. The unfavorable interaction between the isopropyl group on the oxazolidinone and the approaching phenyl ring of benzaldehyde appears to be quite high in **TS-*a*-A$_2$**. In **TS-*a*-S$_1$** and **TS-*a*-S$_2$**, the methyl group of the titanium enolate is found to be at a favorable distance from the phenyl ring to enable weak CH···π interactions.[38] Interestingly, all TSs leading to *anti* aldol products lack CH···π interactions owing to the relative orientations of the phenyl and the methyl groups (Figure 1). Another weak interaction between the axial chloride ligands of titanium and the methylene hydrogens of the oxazolidinone ring is also

(36) (a) Behnam, S. M.; Behnam, S. E.; Ando, K.; Green, N. S.; Houk, K. N. *J. Org. Chem.* **2000**, *65*, 8970. (b) Janardanan, D.; Sunoj, R. B. *Chem.—Eur. J.* **2007**, *13*, 4805. (c) Janardanan, D.; Sunoj, R. B. *J. Org. Chem.* **2008**, *73*, 8163.

(37) In fact, the initial guess geometry with a chair-like conformation has been identified to converge into a boat-like arrangement during the geometry optimization of the transition states.

(38) (a) The shortest contact distances of CH···π interactions are identified as 2.79 and 2.74 Å respectively in **TS-S$_1$** and **TS-S$_2$**. (b) These distances fit well within the range of CH···π contacts usually reported in literature. (c) Takahashi, O.; Kohno, Y.; Saito, K.; Nishio, M. *Chem.—Eur. J.* **2003**, *9*, 756. (d) Suezawa, H.; Ishihara, S.; Umezawa, Y.; Tsuboyama, S.; Nishio, M. *Eur. J. Org. Chem.* **2004**, 4816.

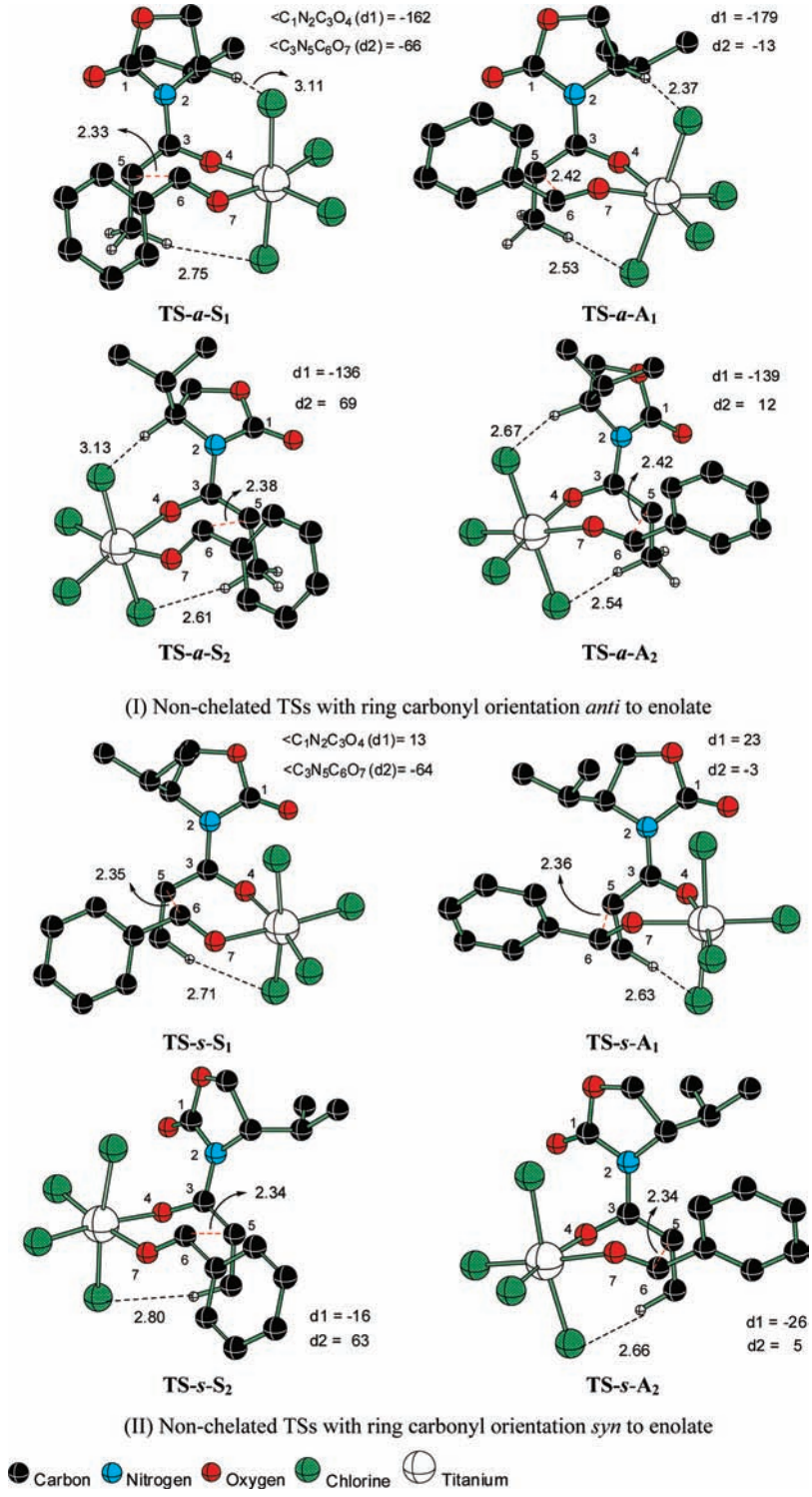

Figure 1. B3LYP/6-31G* optimized geometries of lower energy diastereomeric transition states in the nonchelated pathway for the addition of titanium enolate to benzaldehyde with oxazolidinone (**1a**) as the chiral auxiliary. Only selected hydrogens are shown for clarity. The distances are in Å.

noticed. The CH···Cl distances are found to be in the range of 2.53−2.75 Å. A number of weak interactions between aldehydic or enolate hydrogens and the chloride ligands or the ring carbonyl are also identified. A pictorial representation of all these weak interactions and the calculated electron densities at the corresponding bond critical points are provided in the Supporting Information.[39] The calculated dipole moments of the TSs are also found to exhibit good correlation with the observed selectivity, wherein the lowest energy TS is identified to have the lowest dipole moment.[40] The cumulative effect of the above-mentioned weak interactions will contribute to the vital energy difference between the diastereomeric TSs required for imparting high levels of stereoselectivity. Moreover, we have carried out distortion−interaction analysis of the key TSs to gain improved insight into the origin of stereoselectivity (*vide infra*).

The energies of TSs wherein the ring carbonyl orientation is *syn* to the enolate carbonyl (as in Scheme 3-I) are found to be much higher than when the ring carbonyl is *anti* to the enolate

carbonyl. The repulsion between the thiocarbonyl and the enolate carbonyl is expected to become stronger in the case of thiocarbonyl (**1b** and **1c**).[41] Other interactions that help stabilize the TSs are found to be either absent or weak in this model.[42] The oxazolidinone ring in **TS-*s*-S$_1$** and **TS-*s*-S$_2$** is found to remain relatively more coplanar with the enolate. The substituents around the developing C−C bond are in a staggered arrangement (Figure 1-II). The stronger dipolar interaction between the ring and enolate carbonyls in the *syn* arrangement could as well destabilize these TSs. The calculated dipole moments for these TSs are found to be larger.[43] For instance, the dipole moment of **TS-*a*-S$_1$** is only 9.8 D, while the corresponding value is 17.6 D for **TS-*s*-S$_1$**. From these trends it is evident that the TSs prefer a dipole-minimized orientation of the chiral auxiliary. Hence, in oxazolidinone-mediated aldol reactions, the dipole effects likely exert a dominant control on the π-facial selectivity in carbonyl addition reactions.[44]

The analyses of the stereoselectivity-determining TSs, as presented in the above sections, convey that the nonchelated TS model can readily explain the formation of Evans *syn* aldol product through **TS-*a*-S$_1$**.[1a,10] It is of further significance that the predicted trends at the different levels of theory employed in the present study (L1−L7) are in good agreement with the experimental selectivities, besides being mutually consistent. Moreover, the trends remained the same as in Table 1 when the critical TSs were reoptimized by using a 6-311G** basis set.[45]

Until now, the discussions have focused on the importance of nonchelated TSs toward rationalizing the stereochemical outcome, such as the formation of Evans *syn* aldol product. It is of high significance to consider that the product stereochemistry can be quite different if the reaction conditions are altered. Among the key modifications to the reaction conditions, changes in the nature and amount of Lewis bases appear more common.[10] More importantly, interesting changes in stereoselectivity have been reported for Evans oxazolidinone-mediated aldol reactions.[6,9a,10a,c,12] In one such fine example, Crimmins and co-workers illustrated a stereodivergent *syn* aldol reaction by changing the number of equivalents of base. The use of 1 and 2 equiv of base respectively led to the formation of non-Evans *syn* and Evans *syn* aldol products while the rest of the reaction conditions were kept the same. In several of these situations, the involvement of a chelated TS is invoked, although verifications of such models remain largely unavailable in the literature.

The chelation of a chiral auxiliary through carbonyl/thiocarbonyl groups with titanium is possible when a vacant coordination site is created by the removal of one of the chloride ligands. Different scenarios can be envisaged in this context. The base-promoted enolization of $TiCl_4$-bound propionyl oxazolidinone can first lead to an anionic intermediate (**I**), as shown in Scheme 1. The protonated base thus produced can subsequently assist in the removal of the chloride ion. The open coordination site can then be occupied by the carbonyl group, leading to a neutral chelated $TiCl_3$-bound enolate. In the absence of such coordinating groups, the formation of anionic titanium enolate is reported to be favored over that of neutral titanium enolate.[46] When 2 equiv of base is used, it is quite likely that the base can compete for the vacant coordination site, thereby reducing the chances of chelation with the ring carbonyl (or thiocarbonyl) group. In an effort to establish the significance of chelated TS models and the accompanying changes in the stereochemical outcome, we have investigated the reaction between *N*-propionyloxazolidinone and benzaldehyde. Unlike in the nonchelated TS model, the number of rotameric possibilities in the chelated TSs is far too limited due to the presence of additional chelation. The key possibilities for the addition of enolate to benzaldehyde, along with the corresponding stereochemical descriptions, are presented in Scheme 4.

The major difference between the chelated and nonchelated models relates to the orientation of the *N*-propionyloxazolidinone ring in the TS. The chiral auxiliary is rotated by about 180° as a result of the chelation. More significantly, the chelation leads to an interchange of the hindered and unhindered prochiral faces of the enolate with respect to the approaching electrophile.[47] The key TSs for the stereoselectivity-controlling C−C bond formation step for **1a**−**c** have been identified. The barrier for rotation about the N−C bond for the conversion of nonchelated to chelated enolate is found to be only about 2−3 kcal/mol for the chiral auxiliaries examined in this study.[48] Hence, under the standard reaction conditions, rotation about the N−C bond can result in reversal of the prochiral face offered by the oxazolidinone-tethered enolate. However, in the case of thiocarbonyl coordination, as in **1b** and **1c**, more effective chelation and additional stabilization of the enolate complex is likely.[49]

The computed relative energies of important diastereomeric TSs in the chelated pathway are provided in Table 2. It can be readily noticed that the lowest energy TS is **TS-S$_2$′**, which is responsible for the formation of non-Evans *syn* aldol product **S$_2$**. This is found to be true for all three chiral auxiliaries. More interestingly, the predicted stereochemical outcome is in full accord with the experimental observations.[10] The energy difference between the lower energy diastereomeric TSs (**TS-S$_2$′** and **TS-A$_2$′**) is found to vary, depending on the nature of the heteroatom present in the chiral auxiliary, alluding to a possible

(39) (a) See Figure S3 and Table S2 in the Supporting Information. (b) The topological analysis of electron densities are carried out by using Bader's Atom-in-Molecule formalism and was carried out by using AIM2000 software. (c) Bader, R. F. W. *Atoms in Molecules: A Quantum Theory*; Clarendon Press: Oxford, 1990. (d) *AIM2000*, Version 2.0; The Buro fur Innovative Software, SBK-Software: Bielefeld, Germany, 2000.

(40) Calculated dipole moments for all the TSs are tabulated in Table S3 of the Supporting Information. A representative set of TSs is also provided to depict the direction of the dipole in Figure S5.

(41) In fact, this is reflected in our attempts to optimize some of the TSs in this category. Even after repeated attempts we were able to optimize only the TSs leading to *syn* products (**S$_1$** and **S$_2$** for oxazolidinethione, and **S$_2$** for thiazolidinethione). All other initial guess geometries reverted back, during the course of geometry optimization, to an *anti* orientation, where the ring thiocarbonyl remains *anti* to the enolate oxygen.

(42) The TSs lack stabilizing weak interactions between the ring carbonyl of enolate and the substrate hydrogens; see Figure S3 in the Supporting Information.

(43) The dipole moment values are tabulated in Table S7 in the Supporting Information.

(44) Wipf, P.; Jung, J.-K. *Chem. Rev* **1999**, *99*, 1469.

(45) The relative energies with respect to the lowest energy TS obtained by using the triple-ζ basis set are provided in Table S4 in the Supporting Information.

(46) Marrone, A.; Renzetti, A.; Maria, P. D.; Gérard, S.; Sapi, J.; Fontana, A.; Re, N. *Chem.—Eur. J.* **2009**, *15*, 11537.

(47) Although nonchelated TS models generated by the rotation of oxazolidinone ring can result in interchange between the hindered and unhindered faces of the enolate, as shown in Figure 1-II, these are found to be much higher in energy.

(48) The geometry of TSs and barriers for ring carbonyl/thiocarbonyl coordination are given in Figure S6 of the Supporting Information.

(49) (a) See Figure S7 in the Supporting Information for plausible reaction pathways for the formation of anionic neutral titanium enolate. (b) Gibbs free energies of formation of chelated enolates are provided in Table S5 in the Supporting Information.

Scheme 4. Important Modes of Addition of Titanium Enolate to Benzaldehyde in the Chelated Pathway: View along the Incipient C−C Bond (Reaction Coordinate)[a]

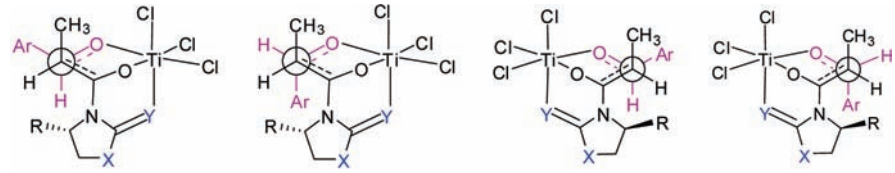

S_1' *re→si* **A_1'** *re→re* **S_2'** *si→re* **A_2'** *si→si*

1a → X=Y=O

1b → X=O, Y=S R = *i*-Pr

1c → X=Y=S

[a] The stereochemical description conveys the mode of addition of the enolate on aldehyde.

Table 2. Computed Relative Energies[a] (kcal/mol) of Important Transition States in the Chelated Pathway Obtained at Various Levels of Theory[b] for the Addition of Titanium Enolate to Benzaldehyde

transition state	mode of approach	relative energy						
		L1	L2	L3	L4	L5	L6	L7
				Oxazolidinone (**1a**)				
TS-S_1'	*re→si*	2.7	3.3	2.8	2.7	2.5	2.6	1.0
		(3.4)	(3.8)	(2.9)	(3.5)	(4.2)	(2.9)	(1.6)
TS-A_1'	*re→re*	3.9	4.0	3.7	3.8	2.6	3.5	1.7
		(4.9)	(3.4)	(3.6)	(4.1)	(3.5)	(3.6)	(1.6)
TS-S_2'	*si→re*	0.0	0.0	2.0	0.0	0.0	0.0	0.5
		(0.0)	(0.6)	(0.9)	(0.8)	(1.4)	(0.4)	(0.0)
TS-A_2'	*si→si*	2.2	2.1	0.0	2.0	0.8	2.0	0.0
		(1.8)	(0.0)	(0.0)	(0.0)	(0.0)	(0.0)	(0.8)
				Oxazolidinethione (**1b**)				
TS-S_1'	*re→si*	2.2	3.1	3.1	2.9	1.3	3.0	0.9
		(2.8)	(7.8)	(2.7)	(2.6)	(3.1)	(2.9)	(2.3)
TS-A_1'	*re→re*	2.9	3.8	3.8	3.5	1.8	3.4	1.2
		(3.1)	(8.3)	(3.5)	(3.0)	(2.5)	(3.2)	(1.3)
TS-S_2'	*si→re*	0.0	0.0	0.0	0.0	0.3	0.0	0.2
		(0.3)	(0.0)	(0.1)	(0.03)	(0.8)	(0.3)	(1.2)
TS-A_2'	*si→si*	1.2	2.2	2.2	1.8	0.0	1.9	0.0
		(0.0)	(4.8)	(0.0)	(0.0)	(0.0)	(0.0)	(0.0)
				Thiazolidinethione (**1c**)				
TS-S_1'	*re→si*	3.4	3.7	6.5	3.4	4.3	1.0	2.3
		(2.8)	(2.6)	(6.1)	(2.6)	(1.8)	(1.9)	(2.7)
TS-A_1'	*re→re*	3.7	3.9	3.9	3.6	2.3	3.4	1.2
		(3.3)	(2.8)	(3.5)	(3.2)	(2.7)	(3.1)	(0.4)
TS-S_2'	*si→re*	0.0	0.0	0.0	0.0	0.0	0.0	0.0
		(0.0)	(0.0)	(0.0)	(0.0)	(0.0)	(0.0)	(0.0)
TS-A_2'	*si→si*	2.4	2.8	2.7	2.3	1.7	2.3	0.9
		(1.0)	(0.2)	(0.9)	(1.1)	(0.4)	(1.1)	(0.1)

[a] L1 = $PCM_{(DCM)}$/B3LYP/6-311+G**//B3LYP/6-31G*; L2 = $PCM_{(DCM)}$/mPW1K/6-311+G**//mPW1K/6-31G*; L3 = $PCM_{(DCM)}$/mPW1PW91/6-311+G**//mPW1PW91/6-31G*; L4 = $PCM_{(DCM)}$/B3LYP/LANL2DZ (Ti), 6-311+G**//B3LYP/LANL2DZ (Ti), 6-31G* for all other atoms; L5 = $PCM_{(DCM)}$/M05-2X/6-311+G**//M05-2X/6-31G*; L6 = $PCM_{(DCM)}$B98/6-311+G**//B98/6-31G*; L7 = $COSMO_{(DCM)}$/B3LYP-D/6-311+G**//B3LYP/6-31G*. [b] Gas-phase relative energies at respective levels of theory are given in parentheses.

change in the stereochemical outcome by varying the chelation around the titanium center. Subtle changes in the chelation ability of the heteroatom or the use of other substrates bearing functional groups capable of chelation with the titanium might bring about interesting changes in the stereoselectivity.[50] Insights of this kind could perhaps be made use of in rational modification of chiral auxiliaries.

The optimized geometries of a representative set of diastereomeric TSs in the case of thiazolidinethione are provided in Figure 2.[51] The octahedral coordination topology around the titanium in the chelated TSs is found to be more distorted as compared to that in the nonchelated TSs.[52] It can be noticed that axial ligands such as thiocarbonyl and chloride remain nonlinear and result in a distorted octahedral geometry. The TSs

(50) Shinisha, C. B.; Sunoj, R. B. *Org. Lett.* **2010**, *12*, 2868.

(51) The optimized geometries of the diastereomeric chelated transition states for **1a** and **1b** are given in Figure S8 in the Supporting Information.

(52) Similar observations are reported earlier with titanium complexes possessing bidentate ligands. See: (a) Reetz, M. T. *Acc. Chem. Res.* **1993**, *26*, 462. (b) Jonas, V.; Frenking, G. *Organometallics* **1993**, *12*, 2111. (c) Jonas, V.; Frenking, G.; Reetz, M. T. *Organometallics* **1995**, *14*, 5316.

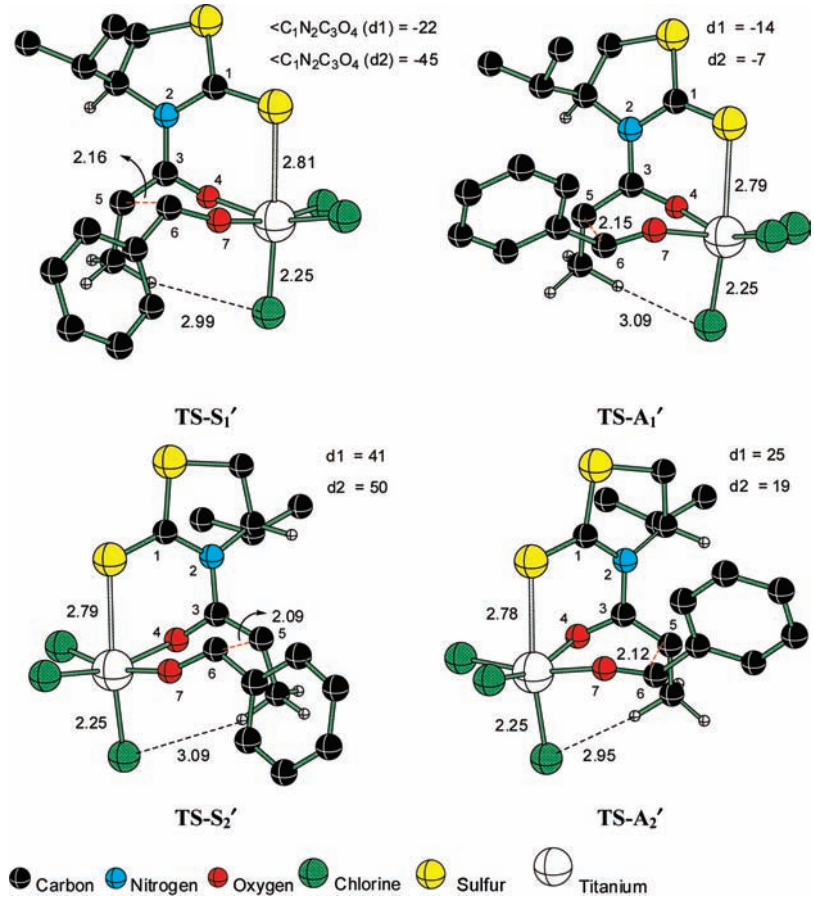

Figure 2. B3LYP/6-31G* optimized geometries of lower energy diastereomeric transition states in the chelated pathway for the addition of titanium enolate to benzaldehyde with thiazolidinethione (**1c**) as the chiral auxiliary. Only selected hydrogens are shown for clarity. The distances are in Å.

leading to Evans (**TS-S$_1$′**) and non-Evans *syn* aldol (**TS-S$_2$′**) products exhibit a chair-like geometry, similar to that noticed earlier in the nonchelated pathway. The phenyl group of benzaldehyde in both **TS-S$_1$′** and **TS-S$_2$′** is farther from the chiral auxiliary. In addition to such geometric features that help minimize steric interactions, the phenyl group tends to remain at a favorable distance (~2.75 Å) to develop C−H···π interaction with the methyl group of the enolate. In the boat-like TSs, such as in **TS-A$_1$′** and **TS-A$_2$′**, which are responsible for *anti* aldol products, C−H···π stabilizing interactions are absent owing to the orientation of the phenyl group.[31,53] The analysis of various factors that influence the relative energies indicates subtle and interesting variations between these TSs. Among the four lower energy TSs, **TS-A$_1$′** leading to Evans *anti* aldol is found to be the highest energy TS. The steric interaction between the phenyl group and the isopropyl group of the chiral auxiliary appears to be the major contributor in this case. The facial selectivity is largely influenced by the substituent on the chiral auxiliary ring. In fact, there have been reports on the use of different substituents at the fourth position of the chiral auxiliary ring.[11] The relative energies computed by using the optimized geometries with a more flexible triple-ζ-quality basis set are also found to be in good agreement with the results presented here.[54]

A detailed comparison of the geometric features between chelated and nonchelated TSs is presented in Table 3. The Ti···O═C$_{enolate}$ bond length in TSs is generally elongated as compared to that in the corresponding PRCs in both nonchelated and chelated pathways.[55] The efficiency of donation of an enolate oxygen lone pair to the empty d-orbitals of titanium is found to get weaker upon coordination with benzaldehyde. As the C−C bond formation completes, the bond between the oxygen of benzaldehyde and titanium becomes progressively shorter. In accordance with the expectations, further elongation of the Ti···O═C$_{enolate}$ distance toward the product side can be noticed as well. In the chelated TSs, stronger Ti···Y═C donor−acceptor interaction is found to weaken the Ti···O═C$_{enolate}$ interaction. For instance, in the case of **1a** leading to product **S$_2$**, the Ti···O═C$_{enolate}$ distance increases from 1.86 Å in the PRC to 2.29 Å in the resulting intermediate toward the product side. In the chelated TSs, an interesting difference between the coordination of carbonyl and thiocarbonyl is noticed. Upon going from TS to product, the enolate coordination breaks in the case of **1a**, whereas it remains intact in **1b** and **1c**. In the latter cases, however, the coordination of the ring thiocarbonyl is found to be absent.

(53) Zhao, Y.; Truhlar, D. G. *J. Phys. Chem. A* **2005**, *109*, 5656.
(54) The relative energies computed using geometries optimized with the 6-311G** basis set at the levels of theory L1−L6 are provided in Table S6 in the Supporting Information.
(55) The pre-reacting complexes (PRCs) and succeeding intermediates (Int) are identified using the intrinsic reaction coordinate (IRC) calculations starting from the respective TSs. The last point, as obtained through the IRC runs, has been subjected to further geometry optimization using the 'opt = calcfc' option available in the program. The stationary points thus obtained are characterized as true minima by using additional frequency calculations.

Table 3. Comparison of Key Structural Parameters for Chelated and Nonchelated Transition States, Pre-reacting Complexes, and Succeeding Intermediates Obtained at the B3LYP/6-31G* Level of Theory (Distances in Å)

			bond lengths with titanium				
			nonchelated TSs		chelated TSs		
transition state	chiral auxiliary		···O═$C_{enolate}$	···O═C_{PhCHO}	···O═$C_{enolate}$	···O═C_{PhCHO}	···Y═C[a]
TS-S_1	**1a**	PRC	1.86	2.26	1.85	2.31	2.15
		TS	2.03	2.04	2.06	1.94	2.31
		Int	2.40	1.81	4.68	1.76	2.28
	1b	PRC	1.86	2.26	1.85	2.26	2.64
		TS	2.05	2.01	2.03	1.94	2.84
		Int	2.41	1.81	2.25	1.78	4.89
	1c	PRC	1.85	2.27	1.85	2.26	2.65
		TS	2.07	2.00	2.02	1.94	2.81
		Int	2.43	1.81	2.24	1.78	4.81
TS-A_1	**1a**	PRC	1.84	2.27	1.86	2.28	2.30
		TS	2.03	2.03	2.07	1.97	2.31
		Int	4.38	1.77	3.67	1.77	2.27
	1b	PRC	1.84	2.26	1.85	2.26	2.64
		TS	2.05	2.01	2.03	1.97	2.82
		Int	4.28	1.77	2.25	1.77	4.88
	1c	PRC	1.86	2.26	1.85	2.26	2.65
		TS	2.07	1.99	2.03	1.97	2.80
		Int	4.34	1.77	2.25	1.77	4.88
TS-S_2	**1a**	PRC	1.86	2.26	1.85	2.24	2.17
		TS	1.99	2.06	2.08	1.93	2.29
		Int	2.29	1.82	5.38	1.75	2.26
	1b	PRC	1.81	2.31	1.83	2.28	2.61
		TS	2.02	2.04	2.06	1.93	2.81
		Int	2.31	1.82	2.34	1.81	3.06
	1c	PRC	1.82	2.31	1.84	2.27	2.65
		TS	2.04	2.04	2.06	1.94	2.79
		Int	2.31	1.82	2.45	1.80	2.97
TS-A2	**1a**	PRC	1.81	2.31	1.86	2.28	2.15
		TS	2.01	2.05	2.07	1.96	2.29
		Int	2.43	1.81	3.83	1.76	2.29
	1b	PRC	1.82	2.39	1.84	2.27	2.65
		TS	2.05	2.03	2.04	1.95	2.81
		Int	4.31	1.78	2.26	1.78	4.99
	1c	PRC	1.82	2.39	1.84	2.26	2.65
		TS	2.07	2.03	2.04	1.95	2.78
		Int	2.27	1.80	2.26	1.77	4.98

[a] Y = O for **1a**; Y = S for **1b** and **1c**.

The comparison between the TSs for **1a** and **1c** provides certain interesting details. It is noticed that the chelation in **1c** is more favored because of the longer C═S bond (1.67 Å) as compared to the ring carbonyl (with a C═O bond distance of 1.20 Å) as in **1a**. Such chelation helps to reduce the crowding around the titanium in **1c**. Further, the inherently higher affinity of sulfur for titanium as compared to oxygen favors the chelated pathway in **1c** more than in **1a**.[56] Enhanced preference of titanium toward sulfur over that of a second oxygen ligand (when one of the coordination sites is preoccupied by oxygen) is borne out by NMR experiments on titanium complexes.[57] The ring sulfur, such as in **1c**, may also influence the donor−acceptor interaction between titanium and the exocyclic thiocarbonyl/carbonyl group through electronic interaction. This is evident from the longer distance between titanium and thiocarbonyl sulfur in **1b** than in **1c**. All the above-mentioned stabilizing/destabilizing interactions and the accompanying subtle changes in the TS geometries can safely be regarded as the factors responsible for the variations in the stereochemical outcome with respect to the changes in the nature of chiral auxiliaries.

Distortion and Interaction Analysis. More detailed insights into the trends in the relative energy order between the key TSs are sought by employing the *activation strain* model. The analysis of activation barriers by using this approach could help us understand the origins of stereoselectivity[58] in a more meaningful manner. In this model, the activation energy ($\Delta E^{\ddagger}$) is decomposed into two key terms, distortion and interaction energies. The distortion energy of the reactants ($\Delta E^{\ddagger}_{d}$) is computed as the energy difference between the native unstrained reactant and the corresponding distorted reactant geometries as in the respective TS. The interaction energy ($\Delta E^{\ddagger}_{i}$) is calculated as the binding interaction between these distorted reactants at

(56) In an earlier report Fowles *et al.* reported the preferential coordination of thioxane with titanium through sulfur rather than oxygen: Fowles, G. W. A.; Rice, D. A.; Wilkins, J. D. *J. Chem. Soc. A* **1971**, 1920.

(57) McAlees, A. J.; McCrindle, R.; Woon-Fat, A. R. *Inorg. Chem.* **1976**, *15*, 1065.

(58) Through systematic use of the distortion−interaction model, a deeper understanding of chemical reactions can be achieved in terms of the stereoelectronic changes with the reactants. See: (a) Poirier, R. A.; Pye, C. C.; Xidos, J. D.; Burnell, D. J. *J. Org. Chem.* **1995**, *60*, 2328. (b) Legault, C. Y.; Garcia, Y.; Merlic, C. A.; Houk, K. N. *J. Am. Chem. Soc.* **2007**, *129*, 12664. (c) Ess, D. H.; Houk, K. N. *J. Am. Chem. Soc.* **2008**, *130*, 10187. (d) Lam, Y.-h.; Cheong, P. H.-Y.; Blasco Mata, J. M.; Stanway, S. J.; Gouverneur, V.; Houk, K. N. *J. Am. Chem. Soc.* **2009**, *131*, 1947.

Table 4. Computed Distortion ($\Delta E^{\ddagger}_{d}$)[a] and Interaction ($\Delta E^{\ddagger}_{i}$) Energies[b] (kcal/mol) for the Nonchelated Transition States Obtained at the $PCM_{(DCM)}$/B3LYP/6-311+G**//B3LYP/6-31G* Level of Theory

transition state	$\Delta E^{\ddagger}_{d}$	$\Delta E^{\ddagger}_{d}$(N)	$\Delta E^{\ddagger}_{d}$(E)	$\Delta E^{\ddagger}_{i}$	$\Delta E^{\ddagger c}$
			Oxazolidinone (**1a**)		
TS-a-S$_1$	30.7 (30.7)[b]	23.6 (23.1)	7.1 (7.7)	−27.4 (−29.2)	3.3 (1.6)
TS-a-A$_1$	31.8 (32.6)	26.2 (26.7)	5.6 (6.2)	−25.3 (−27.0)	6.5 (5.9)
TS-a-S$_2$	31.8 (31.4)	26.0 (25.1)	5.8 (6.3)	−23.9 (−24.2)	7.9 (7.2)
TS-a-A$_2$	33.6 (35.9)	27.7 (29.5)	5.9 (6.4)	−24.3 (−26.6)	9.3 (9.3)
			Oxazolidinethione (**1b**)		
TS-a-S$_1$	36.0 (34.6)	27.8 (25.8)	8.2 (8.8)	−29.9 (−31.5)	6.1 (3.1)
TS-a-A$_1$	37.0 (36.6)	30.4 (39.4)	6.6 (7.1)	−26.9 (−28.5)	10.1 (8.1)
TS-a-S$_2$	33.3 (32.0)	27.1 (25.2)	6.3 (6.8)	−23.0 (−23.6)	10.3 (8.4)
TS-a-A$_2$	39.0 (39.9)	31.3 (31.6)	7.8 (8.3)	−27.3 (−29.5)	11.8 (10.5)
			Thiazolidinethione(**1c**)		
TS-a-S$_1$	39.2 (37.5)	30.4 (28.1)	8.8 (9.4)	−31.1 (−32.8)	8.2 (4.8)
TS-a-A$_1$	40.6 (40.1)	33.0 (31.9)	7.6 (8.2)	−28.3 (−30.2)	12.3 (9.9)
TS-a-S$_2$	35.5 (37.3)	29.9 (27.5)	7.4 (7.9)	−25.8 (−26.1)	11.4 (9.4)
TS-a-A$_2$	41.5 (41.9)	33.1 (32.9)	8.4 (9.0)	−28.3 (−30.3)	13.2 (11.6)

[a] Refers to the total distortion energy, consisting of (i) the energy required to distort the geometry of the enolate bound to $TiCl_4$ to the geometry in the TS, denoted as $\Delta E^{\ddagger}_{d}$(N), and (ii) the distortion energy of benzaldehyde, denoted as $\Delta E^{\ddagger}_{d}$(E). [b] Gas-phase energies calculated at the B3LYP/6-311+G**//B3LYP/6-31G* level are given in parentheses. [c] Calculated with respect to titanium enolate and benzaldehyde.

Table 5. Computed Distortion ($\Delta E^{\ddagger}_{d}$)[a] and Interaction ($\Delta E^{\ddagger}_{i}$) Energies[b] (kcal/mol) for the Chelated Transition States Obtained at the $PCM_{(DCM)}$/B3LYP/6-311+G**//B3LYP/6-31G* Level of Theory

transition state	$\Delta E^{\ddagger}_{d}$	$\Delta E^{\ddagger}_{d}$(N)	$\Delta E^{\ddagger}_{d}$(E)	$\Delta E^{\ddagger}_{i}$	$\Delta E^{\ddagger c}$
			Oxazolidinone (**1a**)		
TS-S$_1$′	49.2 (50.5)[b]	34.7 (35.4)	14.4 (15.2)	−39.3 (−40.1)	9.9 (10.4)
TS-A$_1$′	52.2 (47.4)	35.9 (36.3)	16.3 (17.0)	−41.2 (−42.6)	11.0 (10.7)
TS-S$_2$′	51.5 (53.1)	33.4 (34.2)	18.1 (18.8)	−44.4 (−44.6)	7.1 (8.4)
TS-A$_2$′	49.2 (51.0)	33.4 (34.4)	15.8 (16.6)	−39.9 (−42.7)	9.3 (8.2)
			Oxazolidinethione (**1b**)		
TS-S$_1$′	47.0 (46.8)	33.9 (32.9)	13.1 (13.8)	−35.8 (−37.2)	11.2 (9.5)
TS-A$_1$′	49.8 (49.3)	35.2 (33.9)	14.6 (15.3)	−38.0 (−39.7)	11.8 (9.5)
TS-S$_2$′	47.7 (47.0)	32.8 (31.3)	14.9 (15.6)	−39.4 (−39.6)	8.3 (7.4)
TS-A$_2$′	46.8 (46.8)	32.4 (31.6)	14.4 (15.2)	−36.7 (−39.5)	10.1 (7.3)
			Thiazolidinethione (**1c**)		
TS-S$_1$′	45.2 (46.6)	32.4 (33.1)	12.8 (13.5)	−34.8 (−36.6)	10.4 (10.0)
TS-A$_1$′	47.4 (48.4)	33.4 (33.8)	13.9 (14.6)	−36.7 (−38.5)	10.7 (9.9)
TS-S$_2$′	45.4 (46.2)	30.7 (30.8)	14.7 (15.4)	−38.4 (−38.8)	7.0 (7.4)
TS-A$_2$′	44.1 (45.8)	30.5 (31.5)	13.6 (14.3)	−34.7 (−37.5)	9.4 (8.3)

[a] Refers to the total distortion energy consisting of (i) the energy required to distort the geometry of enolate bound to $TiCl_3$ to the geometry in the TS, denoted as $\Delta E^{\ddagger}_{d}$(N), and (ii) the distortion energy of benzaldehyde, denoted as $\Delta E^{\ddagger}_{d}$(E). [b] Gas-phase energies calculated at the B3LYP/6-311+G**//B3LYP/6-31G* level are given in parentheses. [c] Calculated with respect to titanium enolate and benzaldehyde.

the TS geometry. The distortion energy depends on the ability of the reactants to reorganize into their deformed structures in the TS, which is devoid of any interaction between the reactants. The interaction energy, on the other hand, depends on the electronic structure features as well as the relative orientations of the reactants during the bond formation.[59] The results of the activation strain model in terms of *distortion* and *interaction* on the nonchelated TSs are presented in Table 4.

Interesting trends emerge from the analyses of the distortion and interaction energies of stereochemically crucial TSs. A perusal of distortion energies in the case of nonchelated TSs reveals that the contribution to the deformation energy is primarily due to the distortion of the enolate fragment rather than that of benzaldehyde. For instance, with the lowest energy TS (**TS-*a*-S$_1$**), the deformation energies for enolate and benzaldehyde are respectively 23.6 and 7.1 kcal/mol. Similarly, the stabilizing interactions are also found to exhibit interesting variations. In the case of all three chiral auxiliaries, higher stabilizing interaction energy is noticed for the TSs responsible for the formation of Evans *syn* aldol. The $\Delta E^{\ddagger}_{i}$ value is −27.4 kcal/mol for the lowest energy TS (**TS-*a*-S$_1$**), whereas it is −25.3 kcal/mol for the next higher energy TS (**TS-*a*-A$_1$**) for oxazolidinone-mediated C−C bond formation. Most strikingly, the net balance between the destabilizing distortion and stabilizing interaction energies is found to follow the predicted energy order between the diastereomeric TSs. In other words, the agreement between the predicted trends in stereoselectivity is consistent with the preferred order as given by the activation strain model. With each of the chiral auxiliaries, the lowest energy TS exhibits the highest $\Delta E^{\ddagger}_{i}$ value. It is therefore highly suggestive that the key to the higher stability of **TS-*a*-S$_1$** stems from the improved interaction energy between the reacting partners. In this TS, the unhindered face of the enolate adds to benzaldehyde through a chair-like geometry; with a staggered arrangement of the substituents around the incipient C−C bond, the maximum stabilizing interaction energy is noticed. A closely related analysis is also carried out on the PRC preceding each stereochemically unique TS for the addition of nucleophile to electrophile. The distortion and interaction energies in these PRCs capture effects due to the ligand reorganization accompanying the formation of a hexacoordinate titanium. In general, the stabilizing interaction energy between the reactants is found to be more than the destabilizing deformation energies in PRCs.[60] This could be regarded as responsible for the improved stability of the PRCs as compared to the separated reactants.

The distortion and interaction energy analysis for the C−C bond formation involving chelated TSs is also performed. The results are summarized in Table 5. The crucial difference here, as compared to the nonchelated pathway, is that the ring carbonyl/thiocarbonyl chelation renders higher rigidity to the titanium complex. As with the nonchelated TSs, higher distortion energy is noticed for the titanium enolate moiety as compared to that in benzaldehyde. More importantly, the distortion of benzaldehyde is found to be more in the chelated TSs. For instance, the distortion energy of benzaldehyde leading to the formation of product **S$_1$** is 7.1 kcal/mol in the nonchelated TS, while it is as high as 14.4 kcal/mol in the chelated TS. The interaction energy indeed plays a key role in determining the relative stabilization of the TSs. In all three chiral auxiliaries, the value of $\Delta E^{\ddagger}_{i}$ for **TS-S$_2$′** is found to be the highest. This implies that the TS responsible for the formation of non-Evans *syn* aldol product (**S$_2$**) enjoys the highest stabilizing interaction energy as compared to the other three stereochemically competing TSs. The chair-like C−C bond formation TS geometry, involving the attack of the unhindered face of the enolate on benzaldehyde with a staggered arrangement of the substituents around the developing C−C bond, facilitates improved interaction energy between the fragments. The net effect of these

(59) (a) Diefenbach, A.; Bickelhaupt, F. M. *J. Phys. Chem. A* **2004**, *108*, 8460. (b) de Jong, G. T.; Visser, R.; Bickelhaupt, F. M. *J. Organomet. Chem.* **2006**, *691*, 4341. (c) de Jong, G. T.; Bickelhaupt, F. M. *Chem. Phys. Chem.* **2007**, *8*, 1170. (d) de Jong, G. T.; Bickelhaupt, F. M. *J. Chem. Theory Comput.* **2007**, *3*, 514. (e) Fernández, I.; Bickelhaupt, F. M.; Cossío, F. P. *Chem.—Eur. J.* **2009**, *15*, 13022.

(60) Complete details of distortion−interaction analysis are provided in Table S8 in the Supporting Information.

factors and the predicted trends are certainly in agreement with the energy ordering between the TSs, as noticed in the present case.

The computed activation barriers for the C−C bond formation ($\Delta E^{\ddagger}_{act}$), respectively for nonchelated and chelated pathways, are provided in Tables 4 and 5. It is evident that the destabilizing distortion energies dominate over the gain in stability due to the interaction energies. This results in positive activation barriers for the C−C bond formation. However, in the case of PRCs, the stabilizing interaction energy is higher than the distortion energy, leading to a net stabilization of the PRCs with respect to the corresponding reactants.[61] Comparison of the activation barriers between chelated and nonchelated pathways readily reveals that the barriers for the latter are lower. Interestingly, this prediction is along the similar lines as that of an earlier experimental observation by Das and Thornton, wherein the improved speed in a series of diastereoselective aldol reactions between chiral lithium enolate and ketones was attributed to the involvement of a nonchelated TS.[62] It can be further noticed that the barriers associated with **1a**, in both chelated and nonchelated pathways, are lower than those for the other chiral auxiliaries, **1b** and **1c**. Hence, under normal conditions, the reaction is likely to proceed through a nonchelated pathway leading to Evans *syn* aldol as the major product. However, under suitably modified reaction conditions (*vide supra*), the displacement of one of the chloride ions can facilitate the coordination of the ring carbonyl (**1a**) or thiocarbonyl (**1b** and **1c**) to titanium. Such changes can lead to non-Evans *syn* aldol as the major product. It is therefore evident from the present study that the stereodivergence in the chiral auxiliary-mediated asymmetric aldol reaction between titanium enolate and benzaldehyde can be rationalized by using suitable chelated and nonchelated TS models.

The TS models described in this study can shed light on the origin of stereoselectivity and other potential factors capable of influencing the stereochemical outcome of titanium enolate-promoted aldol reactions. The details of the stereoelectronic effects illustrated herein could be applied toward gaining valuable insights on the mechanistic implications of Evans oxazolidinone as well as other chiral auxiliary-mediated reactions.[50]

Conclusion

The titanium(IV)-promoted aldol reaction between propionyl oxazolidinone and benzaldehyde has been investigated with the help of density functional theory calculations. Other commonly employed oxazolidinone variants such as oxazolidinethione as well as thiazolidinethione have also been examined. Both chelated and nonchelated transition states have been identified for all the stereochemically important modes of addition between titanium enolate and electrophile. The relative energies of the stereoselectivity-determining TSs are found to be effective toward rationalizing the formation of Evans *syn* and non-Evans *syn* aldol products. In the nonchelated TS pathway, the attack by the less hindered *re* face of titanium enolate on the *si* face of benzaldehyde is found to be energetically the most favored mode of addition, leading to Evans *syn* aldol product. The calculated energy differences of more than 2 kcal/mol between the vital diastereomeric TSs in each of the systems reported herein concur with the experimentally known diastereomeric excess of >90% toward Evans *syn* aldol product. The cumulative effects of steric, electronic, conformational, and electrostatic factors are found to be effective in rationalizing the relative energy order between the critical diastereomeric TSs controlling the stereochemical outcome of the title reaction. Furthermore, in-depth analysis of the TSs by using the *activation strain model* revealed that the balance between the interaction and distortion energies in stereochemically different modes of approach is a crucial controlling factor responsible for the vital differential stabilization of TSs, and hence to the stereochemical outcome. The facial selectivity is found to be largely influenced by the C_4-substituent, such as an isopropyl group, on the chiral auxiliary. The ring carbonyl or thiocarbonyl chelation with titanium is identified as favoring the formation of neutral titanium enolate. In the chelated TS models, attack by the less hindered *si* face of enolate on the *re* face of benzaldehyde is found to be the favored pathway and results in the formation of non-Evans *syn* aldol product. Further, the steric crowding of ligands around titanium is found to be relatively higher in the case of oxazolidinone as compared to that in oxazolidinethione and thiazolidinethione. The longer C═S···Ti coordinating distance together with the inherently longer C═S bond favors the involvement of a chelated pathway for thiazolidinethione more than that for oxazolidinone. The results are tested across different levels of theory. Gratifyingly, the trends are found to be not only mutually consistent but also in good concurrence with the experimental observations. The results offer a meaningful rationalization of the factors affecting the relative stabilizations of chelated and nonchelated TSs for the critical stereoselectivity-controlling step.

Acknowledgment. Generous computing time from the IIT Bombay computer center as well as Center for Modeling Simulation and Design (CMSD) Hyderabad is gratefully acknowledged. S.C.B. acknowledges a senior research fellowship from CSIR New Delhi and Chandan Patel (IIT Bombay) for valuable suggestions.

Supporting Information Available: Total electronic energies, optimized coordinates of all the transition state geometries, Figures S1−S8, Tables S1−S9, and complete ref 21. This material is available free of charge via the Internet at http://pubs.acs.org.

JA101913K

(61) The deformation interaction analyses done on the PRCs leading to chelated TSs are tabulated in Table S9 in the Supporting Information. The stabilizing interactions between the reactants are again found to dominate over the distortion energies, resulting in net stabilization of the PRCs.

(62) Das, G.; Thornton, E. R. *J. Am. Chem. Soc.* **1993**, *115*, 1302.